Presented at the 36th European PV Solar Energy Conference and Exhibition, 9-13 September 2019, Marseille, France

POLYMER-BASED REAR SIDE LIGHT TRAPPING STRUCTURES FOR SILICON-BASED TANDEM SOLAR CELLS

Hubert Hauser, Oliver Höhn, Ralph Müller, Nico Tucher, Kai Mühlbach, Rita Marlene da Silva Freitas, Jan Benick, Martin Hermle, Benedikt Bläsi
Fraunhofer Institute for Solar Energy Systems ISE
Heidenhofstraße 2, 79110 Freiburg, Germany

ABSTRACT: In this study, we investigated potential improvements for polymeric rear side light trapping structures in silicon-based tandem solar cells. The focus is on process variations and a drastic simplification for the realization. We earlier demonstrated an enhancement of the near IR response of a silicon bottom solar cell by such a rear side structure leading to an efficiency gain of 1.9 % absolute to a 33.3 % efficient device. This structure was realized using nanoimprint lithography for the patterning of a diffraction grating together with plasma etching to remove polymeric residues prior to the silver metallization. Now, we investigated the possibility of substituting the plasma etching process by a wet chemical etching process. While external quantum efficiency (EQE) measurements showed the same excellent light trapping, plasma induced damages can be avoided this way. Furthermore, we investigated gold and aluminum as potential alternative to silver as rear side metallization. Among these, silver was found to be the most promising material.
Besides these process variations, we investigated a self-organization process leading to a pseudo-periodic structure with a well-defined and narrow size pitch distribution of polymeric features (self-organized photonic contact). This is based on the phase separation of two immiscible polymers in a solution that is spin coated. After the spin coating and the simultaneous phase separation, one polymer can selectively be removed. EQE measurements of solar cells with such structures showed that very similar results can be expected for this bottom-up process as for the structures realized via NIL. Thus, a photonic light trapping structure can be realized without applying any lithography.
Keywords: Light Trapping, Tandem, Silicon Solar Cell, Nanoimprint Lithography.

1 INTRODUCTION

To tap the full potential of silicon-based tandem solar cells, it is important to implement photon management taking care of the weakly absorbed photons with energies close to the band gap energy of silicon. This holds especially for 2-terminal multi-junction cell architectures, where due to the requirement for current matching light trapping within the silicon bottom cell is extremely important. We have shown the strong leverage of a photonic rear side concept in a previous work, where the efficiency of a triple junction III/V – silicon solar cell was increased by an absolute value of 1.9% to 33.3% just by the incorporation of a diffraction grating [1]. The diffraction grating with a period of 1 µm in this case was realized using interference lithography as mastering technique [2], Roller-Nanoimprint Lithography (NIL) [3,4] with subsequent plasma etching of a polymeric residual layer and finally silver evaporation to establish both a photonic rear side mirror as well as the rear side contact [1].

The rear side architecture of the silicon bottom solar cell consists of planar passivated contact layers (tunnel oxide and doped poly-silicon, TOPCon [5]) onto which the polymeric photonic structure is realized. An essential aspect here is that the poly-silicon surface has to be opened partially allowing the later metallization to contact the solar cell. This structure is schematically shown in Fig. 1.

In the present study, we demonstrate a process variation based on NIL which avoids the plasma etching and thus potential plasma damages. We found that for thin TOPCon layers, the plasma etching of the residual layer leads to a degradation of the passivation quality. Therefore, we developed a wet chemical etching process to remove the approximately 50 nm thick residual layer remaining after the NIL process.

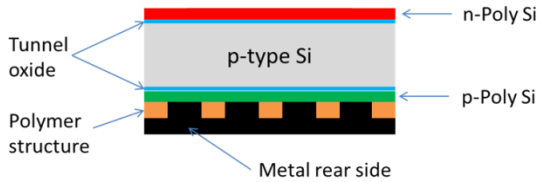

Figure 1: Sketch of the silicon bottom solar cell architecture studied within this work. Polymer residues between structure features have to be removed in order to allow the rear side metallization to contact the solar cell.

To this end we apply the so-called Piranha etching solution (mixture of H_2O_2 and H_2SO_4) [6]. First, we compared the different approaches in optical absorption measurements. Then, simple bottom cell precursors were fabricated and processed using NIL and plasma etching or Piranha etching respectively. EQE measurements were performed and the two methods are compared. Additionally, in this study we compared Ag, Au and Al as potential materials for the rear side metallization.

The diffractive structures described before are periodic crossed gratings with a period of 1 µm, which has been found as optimum period in several works [7–9]. It has been shown that quasi-periodic structures can be realized leading to a ring like scattering profile [10,11]. One interesting process leading to stochastic structures with tunable size and pitch distributions is based on the phase separation of two immiscible polymers in a solution [12,13]. Such structures were already applied to thin film solar cells [14].We realized structures with a pseudo period of approximately 1 µm based on the phase separation of polystyrene (PS) and poly(methyl methacrylate) (PMMA). After the selective removal of the PMMA, the rear side was metallized, resulting in a self-organized photonic contact, and a quantum efficiency measurement was performed.

2 NANOIMPRINT LITHOGRAPHY-BASED APPROACHES

2.1 Processing

Optics samples were made of plain 200 µm thick silicon wafers. Polydimethylsiloxane (PDMS) stamps were replicated from master structures (crossed grating, 1 µm pitch, approx. 250 nm depth) via cast moulding. Diluted SU8 photoresist (1 part SU8-2002, 2 parts Cyclopentanone) was spin coated onto the wafer rear at 5000 rpm. Then a thermally assisted UV-Roller-NIL process was conducted, where the substrate was heated to approx. 100 °C for two minutes to lower the viscosity of the SU8 resist. Then the Roller-NIL process is conducted with a speed of the conveyor belt of ~ 30 cm/min with in-situ UV-curing of the resist. Finally, the substrate is left for two minutes on the heated chuck (still at 100 °C) for the post exposure bake.

After the NIL process, the two processing routes of dry and wet chemical removal of the residual layer were performed. The plasma etching process was conducted in a reactive ion etching (RIE) parallel plate reactor with O_2 (40 sccm) and Ar (50 sccm) as process gases. The pressure is set to 0.05 mbar, the forward power is 100 W, the resulting bias voltage is 200 V and the etching time is 50 s. The wet chemical etching was performed using a mixture of H_2O_2 and H_2SO_4 in a ratio of 1:3. The etching is performed at a temperature of approx. 40 °C for 60 s. Onto these polymeric rear side structures Ag was evaporated thermally.

Solar cell samples were processed on 250 µm thick FZ p-type 1 Ωcm wafers with a HNO_3 tunnel oxide and LPCVD poly-silicon deposited on both sides. On the front an n-type poly-silicon was formed by Phosphorous implantation and on the rear a p-type poly-silicon was formed by Boron implantation. Samples as these were used as bottom cells in multijunction devices; however, here we wanted to characterize them as single junction devices. Therefore, we additionally deposited an AZO / ITO stack on the front side onto which the front side metallization was fabricated by photolithography and lift-off. The rear side gratings were fabricated with both techniques (dry and wet residual layer opening) according to the description of the optics samples. The only difference for the solar cells samples is that prior to the metal deposition on the rear, an HF-Dip was performed to remove the native oxide. Additionally, here besides silver also gold and aluminum was evaporated to investigate their performance as photonic rear side mirror / contact.

2.2 Optical characterization

The optics samples were characterized using a Fourier spectrometer concerning their reflectivity. As there is no transmission for a 2 µm thick rear side metallization, this measurement directly gives insight into the absorption of these samples. SEM inspection into the topography of the two etching approaches showed that for the plasma etching there is a nano-rough resist surface, while the Piranha etching leads to a very smooth surface. This nano-roughness might give rise to an enhanced parasitic absorption.

Fig. 2 shows the absorption determined for a planar reference with Ag metallization as well as samples with rear side gratings processed using dry or wet chemical etching for the residual layer removal.

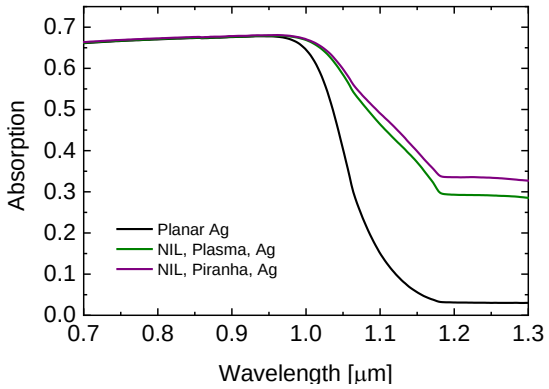

Figure 2: Measured absorption for silicon wafers without ARC with planar rear (black) and the two photonic rear sides with plasma (green) and Piranha etched (violet) residual layer. All samples were metallized using Ag.

It can be seen that both types of photonic rear sides enhance the absorption above 1 µm wavelength drastically compared to the planar reference. The Piranha etched sample even enhances the absorption more than the plasma etched one. However, it can be seen that for both samples with photonic rear there is a considerable part of absorption above 1.2 µm, which can be attributed to parasitic absorption within the metallization as silicon is transparent there. Interestingly, the smooth surface realized using the wet chemical etching leads to the larger amount of parasitic absorption. However, as it is not possible in this stage of characterization to separate between useful and parasitic absorption, it is not possible to conclude, which concept is favorable alone by optical measurements.

2.3 External quantum efficiency measurements

The best possible method to study the light trapping quality of different photonic rear side structures is the measurement of the external quantum efficiency (EQE). Both methods, the wet and the dry etching of the residual layer, were investigated with silver as rear metallization. Additionally, for the wet chemically etched samples we also studied gold and aluminum as potential alternatives for the rear metallization. In Fig. 3 all EQE measurements are shown.

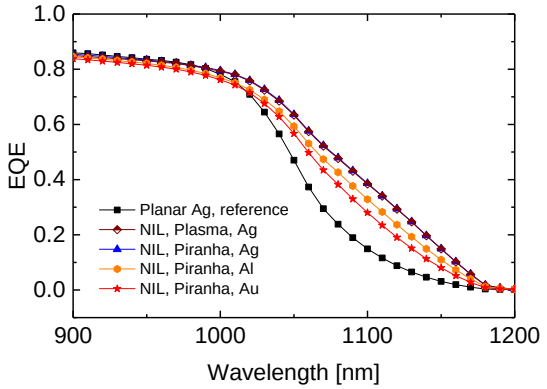

Figure 3: External quantum efficiency (EQE) measurements of samples with different photonic rear side structures.

It can be seen that all photonic rear side structures lead to an improvement of the EQE in the near IR. Furthermore, it can be seen that the plasma etching leads

to virtually the same EQE as the Piranha etched sample. This, together with the fact that the optical absorption measurement showed different results for both samples, highlights the importance of characterizing light trapping structures by means of EQE measurements. The current gain for both methods compared to the planar reference is 1.1 mA/cm², which is in good agreement to the gain already demonstrated in Ref. [1]. Finally, it can be seen that the quality of the photonic rear improves going from gold to aluminum to silver as rear side metallization.

3 SELF-ORGANIZATION OF A POLYMERIC PHOTONIC REAR SIDE

In a further step, we investigated a self-assembly approach to realize a similar polymeric light trapping structure. The phase separation of polymers with different polarity can be used to realize structures with defined and narrow size distribution. Parameters to vary these resulting structure sizes are e.g. molar weights of the polymers, ratio and content of polymers in a solution and spin coating parameters. We investigated solutions made of PMMA and PS in methyl-ethyl-ketone (MEK). After the spin coating process and the occurring phase separation, one polymer phase can selectively be removed (e.g. PMMA in acetic acid). The most important process parameters for the fabrication of this structure are summarized in Table 1.

Table I: Process parameters for the realization of a 1 µm pseudo periodic polymer pattern.

PMMA M_W [$\frac{kg}{mol}$]	PS M_W [$\frac{kg}{mol}$]	Mixing ratio polymers	Polymer Content [wt.%]	Spin speed [rpm]
15	35	1:1	2	1500

Fig. 4 shows an SEM image of a resulting spherical PS structure on a silicon surface. By tuning the processing parameters described before, we managed to fabricate a structure with a pseudo period of approx. 1 µm. This pseudo period was extracted from AFM measurements and a radial auto correlation function (radial ACF).

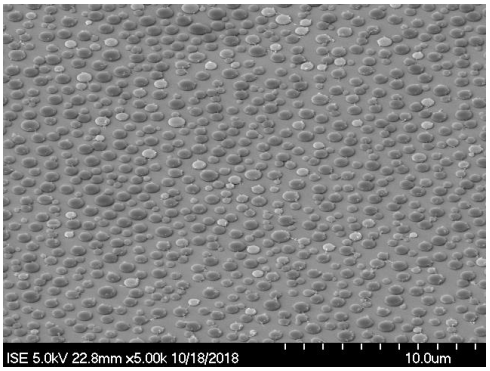

Figure 4: SEM micrograph showing spherical PS particles fabricated in a self-assembly process based on the phase separation of two immiscible polymers.

Again, solar cells were fabricated very similarly to the ones described in section 2.1. However, here the thickness of the samples was 280 µm and there were no TCO layers on top. Therefore, these samples were only suited as EQE samples as IV-parameters would be affected by a too high series resistance. Fig. 5 shows EQE measurements of a solar cell with planar rear and direct silver metallization (planar reference) as well as a sample with the PS polymeric structure and silver metallization. The integrated gain for this structure is approx. 0.7 mA/cm²; however, one has to bear in mind that this value is reached without any ARC. A rescaling of the measurements to exclude front side reflection losses leads to an expected current gain around 1.1 mA/cm². Thus a very similar optical performance can be expected from this self-organized bottom-up structure compared to the well-defined top-down structure realized via NIL.

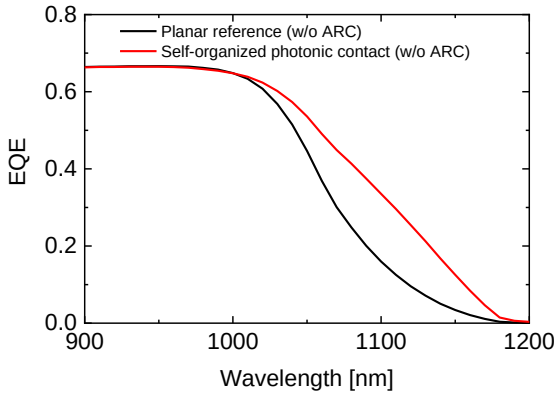

Figure 5: External quantum efficiency (EQE) measurements of a planar reference (black, direct silver metallization on the poly-silicon surface) and a solar cell with a self-organized polymeric structure with subsequent silver metallization on the rear side (self-organized photonic contact) (red). Note that these cells were measured without any ARC.

4 CONCLUSIONS

In this study, we compared different approaches to realize photonic contacts based on polymeric structures on the rear side of silicon-based tandem solar cells. The positive effect of such a structure has been demonstrated before by raising the efficiency of a 2-terminal triple junction III/V on silicon solar cell from 31.4 % to 33.3 % just by enhancing the near IR response of the silicon bottom cell. There, NIL was applied for the patterning of a polymeric structure and plasma etching was applied to remove polymeric residues between the pattern features.

Now, we investigated a potential improvement by changing the etching process of polymeric residues to a wet chemical etching process using a Piranha solution. As expected by this change plasma induced damages in the TOPCon structures can be avoided especially for thin poly silicon layers. The assumption that additionally the decreased nano-roughness of the evaporated metal potentially decreases parasitic absorption could not yet be confirmed as the EQE enhancement was virtually the same.

Furthermore, we present a processing route to realize stochastic polymeric features with a mean pseudo period comparable to the strictly periodic diffraction grating realized by NIL. Here we make use of a phase separation of two immiscible polymers in a solution that is spin coated onto the wafer rear side. After the separation one polymer can selectively be removed. This way we managed to realize a spherical polystyrene (PS) structure

with a pseudo period of approx. 1 µm as targeted for. EQE measurements of solar cells with such polymeric rear side structures showed an integrated current gain, which is comparable to the one reached using NIL. Thus, we demonstrated an easy bottom-up process that can be applied without any lithographic processes to implement a self-organized photonic contact for light trapping in and contacting of silicon-based tandem solar cells.

5 ACKNOWLEDGEMENTS

The authors would like to express their gratitude to Volker Kübler, Sonja Seitz, Felix Schätzle, Frank Dimroth, Felix Predan, Christine Wellens, Adrian Callies at ISE for their support and input in many valuable discussions. This work has received funding from the European Union's Horizon 2020 research and innovation programme within the project SiTaSol under grant agreement No 727497 and by the German Federal Ministry for the Environment, Nature Conservation and Nuclear Safety (Contract Number 0324247, PoTaSi).

6 REFERENCES

[1] R. Cariou, J. Benick, F. Feldmann, O. Höhn, H. Hauser, P. Beutel, N. Razek, M. Wimplinger, B. Bläsi, D. Lackner, M. Hermle, G. Siefer, S.W. Glunz, A.W. Bett, F. Dimroth, III–V-on-silicon solar cells reaching 33% photoconversion efficiency in two-terminal configuration, Nature Energy 17 (2018) 183. https://doi.org/10.1038/s41560-018-0125-0.

[2] A.J. Wolf, H. Hauser, V. Kübler, C. Walk, O. Höhn, B. Bläsi, Origination of nano- and microstructures on large areas by interference lithography, Microelectron Eng 98 (2012) 293–296. https://doi.org/10.1016/j.mee.2012.05.018.

[3] H. Hauser, B. Michl, S. Schwarzkopf, V. Kübler, C. Müller, M. Hermle, B. Bläsi, Honeycomb texturing of Silicon via nanoimprint lithography for solar cell applications, IEEE Journal of Photovoltaics 2 (2012) 114–122. https://doi.org/10.1109/jphotov.2012.2184265.

[4] N. Tucher, O. Höhn, H. Hauser, C. Müller, B. Bläsi, Characterizing the degradation of PDMS stamps in nanoimprint lithography, Microelectronic Engineering 180 (2017) 40–44. https://doi.org/10.1016/j.mee.2017.05.049.

[5] F. Feldmann, M. Bivour, C. Reichel, M. Hermle, S.W. Glunz, Passivated rear contacts for high-efficiency n-type Si solar cells providing high interface passivation quality and excellent transport characteristics, Solar Energy Materials & Solar Cells 120, Part A (2014) 270–274. https://doi.org/10.1016/j.solmat.2013.09.017.

[6] M. Holmes, J. Keeley, K. Hurd, H. Schmidt, A. Hawkins, Optimized piranha etching process for SU8-based MEMS and MOEMS construction, J. Micromech. Microeng. 20 (2010) 1–8. https://doi.org/10.1088/0960-1317/20/11/115008.

[7] A. Mellor, I. Tobias, A. Marti, M.J. Mendes, A. Luque, Upper limits to absorption enhancement in thick solar cells using diffraction gratings, Prog Photovoltaics 19 (2011) 676–687. https://doi.org/10.1002/pip.1086.

[8] I.M. Peters, M. Rüdiger, H. Hauser, M. Hermle, B. Bläsi, Diffractive gratings for crystalline silicon solar cells-optimum parameters and loss mechanisms, Prog. Photovolt: Res. Appl. 20 (2012) 862–873. https://doi.org/10.1002/pip.1151.

[9] N. Tucher, J. Eisenlohr, P. Kiefel, O. Höhn, H. Hauser, I.M. Peters, C. Müller, J.C. Goldschmidt, B. Bläsi, 3D optical simulation formalism OPTOS for textured silicon solar cells, Opt. Express 23 (2015) A1720. https://doi.org/10.1364/oe.23.0a1720.

[10] E.R. Martins, J. Li, Y. Liu, V. Depauw, Z. Chen, J. Zhou, T.F. Krauss, Deterministic quasi-random nanostructures for photon control, Nat Comms 4 (2013) 2665. https://doi.org/10.1038/ncomms3665.

[11] M.-C. van Lare, A. Polman, Optimized Scattering Power Spectral Density of Photovoltaic Light-Trapping Patterns, ACS Photonics 2 (2015) 822–831. https://doi.org/10.1021/ph500449v.

[12] C. Ton-That, A.G. Shard, R.H. Bradley, Surface feature size of spin cast PS/PMMA blends, Polymer 43 (2002) 4973–4977. https://doi.org/10.1016/S0032-3861(02)00333-6.

[13] S. Walheim, M. Böltau, J. Mlynek, G. Krausch, U. Steiner, Structure Formation via Polymer Demixing in Spin-Cast Films, Macromolecules 30 (1997) 4995–5003. https://doi.org/10.1021/ma9619288.

[14] Y.J. Donie, M. Smeets, A. Egel, F. Lentz, J.B. Preinfalk, A. Mertens, V. Smirnov, U. Lemmer, K. Bittkau, G. Gomard, Light trapping in thin film silicon solar cells via phase separated disordered nanopillars, Nanoscale 10 (2018) 6651–6659. https://doi.org/10.1039/C8NR00455B.